Intermediate report
ESRF LT project EC-70
In situ (sub)micro-fluorescence and-diffraction of mantle fluids
and deep-Earth high pressure phases trapped in diamond

K. Janssens, B. Vekemans*, L. Vincze*, F. Brenker**
University of Antwerp, B; *Ghent University, B; **Frankfurt University, D
15/03/08

1. Introduction

Natural diamonds provide the only chemically inert container to bring samples from different depth regions of our Earth up to the surface. In very rare cases these diamonds carry recycled fluids or even ultra deep mantle material (>670km depth). The inclusions provide direct information on the physical and chemical conditions in the deep Earth down to the lower mantle.

In the long-term project, as the first major topic, we exploit a combination of 3D microbeam XRF and of microbeam XRD to obtain so-far inaccessible *in situ* information on the composition of the fluids and the structure and composition of mineral phases present in these extraordinary inclusions in diamonds of various origin. Up to now, diamonds from Finsch and Koffiefontein mines, South Africa have been investigated.

The captured fluids provide us with important information on global recycling processes of various elements along wet subduction zones. Sample locations for deep diamonds are rare, but enclose most of the largest subduction zone systems.

The second topic addressed in this long term project is the study of very small inclusions in diamonds originated from the deepest accessible parts of the Earth, the lower mantle. It is well known that the highest residual pressures can be stored within very small inclusions inside the diamond host. Thus, if their exist any chance to find high pressure phases from the deepest regions of the Earth, this is the best place to look for.

Both types of diamond samples containing fluids or deep mantle material are extremely rare. Due to our succesful previous work, we have access to unique sample material provided by deBeers (Dr. Jeff Harris) and by a private mining company (Dr. F. Kaminsky).

In the table below an overview is given of the measurement periods about which results are reported.

Scheduling period	Beamline(s) Requested	Shifts requested	Results expected (cf. Milestones, §2)
2006 /II	ID18F	21	**Milestone 1** (6 shifts) Characterization of SU8 CRL lenses in the ID18F hardware **Milestone 2** (15 shifts): 2D/3D elemental analysis by confocal XRF imaging and scanning μ-XRD on diamond **inclusions in Juina diamonds originating from the lower mantle** (depth > 670 km) from the alluvial deposit in Mato Grosso, Brazil**. -** emphasis on 2D XRD to select interesting inclusions
2007 /I	ID18F	21	**Milestone 3** (15 shifts): 2D/3D elemental analysis by confocal XRF imaging and scanning μ-XRD studies for structural and **chemical analysis on single fluid inclusion from clouds** in diamonds fromFinsch and Koffiefontein (South Africa).
2007 /II	ID22NI	15	**Milestone 4** (15 shifts): Detailed high resoluiton 2D/3D elemental analysis by confocal XRF imaging studies for chemical analysis on **very small fluid inclusions (<5μm) and the studyof internal details of single inclusions** in lithospheric cloudy diamonds from Finsch and Koffiefontein (South Africa).

2. Milestone 1. Characterization of SU8 CRL lenses at ID18F/XRPD-software.

Next to the use of SU8-CRLs instead of Al-CRLs, in order to reduce the depth range from which information can reach the detector in confocal mode from ca 20 μm to ca 10 μm and with the aim of realising a smaller confocal sampling volume, a more strongly focussing polycapillary lens has been used in front of the fluorescence detector (see Fig. 1).

The size of the sampling volume and associated elemental yield factors were experimentally determined via appropriate standard reference materials. In Fig. w, the dimensions of the primary beam obtainable by means of the SU8-CRL lenses is shown, as well as the relative MDLs achievable in biological and silica-based standard matrices. A primary beam of submicroscopic dimensions can be realised while, depending on the matrix of the material analysed, trace levels at the 10-100 ppb level can be determined.

Additionally an extra XRF detector (drift chamber) has been purchased for integration into the microprobe, allowing simultaneous confocal and conventional XRF measurements. This device, however, has not been installed yet as up to now for our own experimental programme, there was no need to use more than one XRF detector at ID18F.

IDL-based user-friendly μ-XRPD data reduction software that allows for on-line dataviewing and –exploration was developed at the University of Antwerp and has been installed in the ID18F root-directory of the NICE system where it is available for all users of the beamline. The angular resolution in XRPD spectra obtainable at ID18F has been discussed and compared to similar figures-of-merit at other X-ray microprobes in a recently submitted paper:

W. De Nolf, J. Jaroszewicz, R. Terzano, O. Lind, B. Salbu, B. Vekemans, K. Janssens, G. Falkenberg, "X-ray microscopy using synchrotron X-ray powder diffraction with double multilayer and single crystal monochromators", Spectrochimica Acta B (2008).

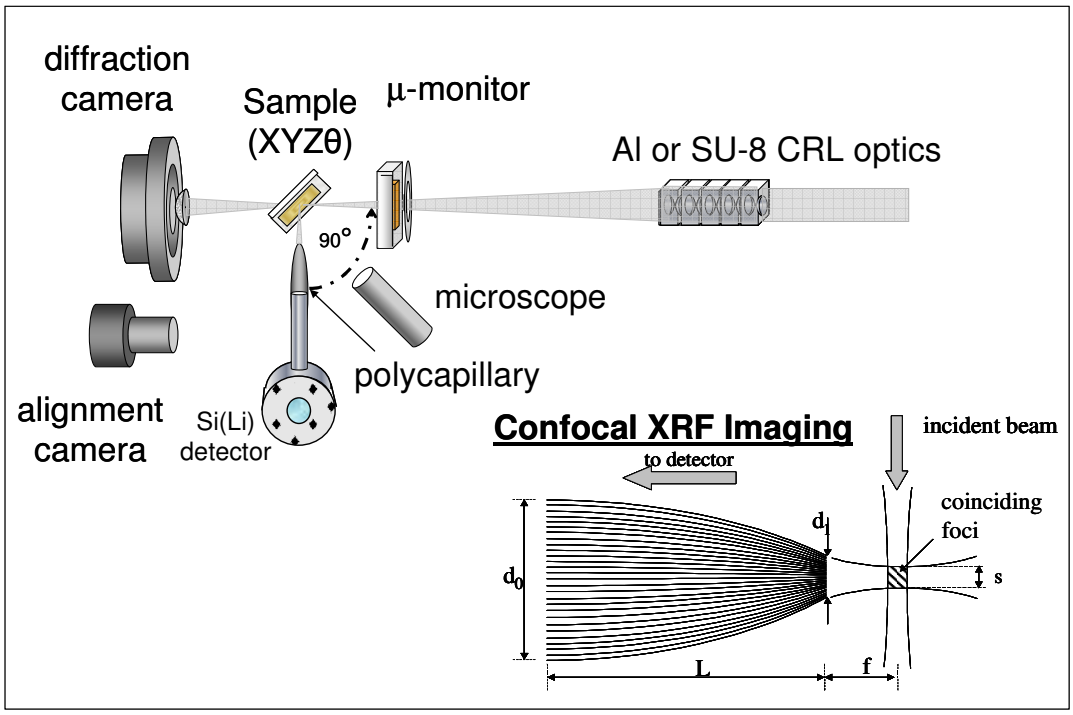

Fig. 1. Experimental setup at ID18F during confocal μ-XRF/μ-XRD experiments

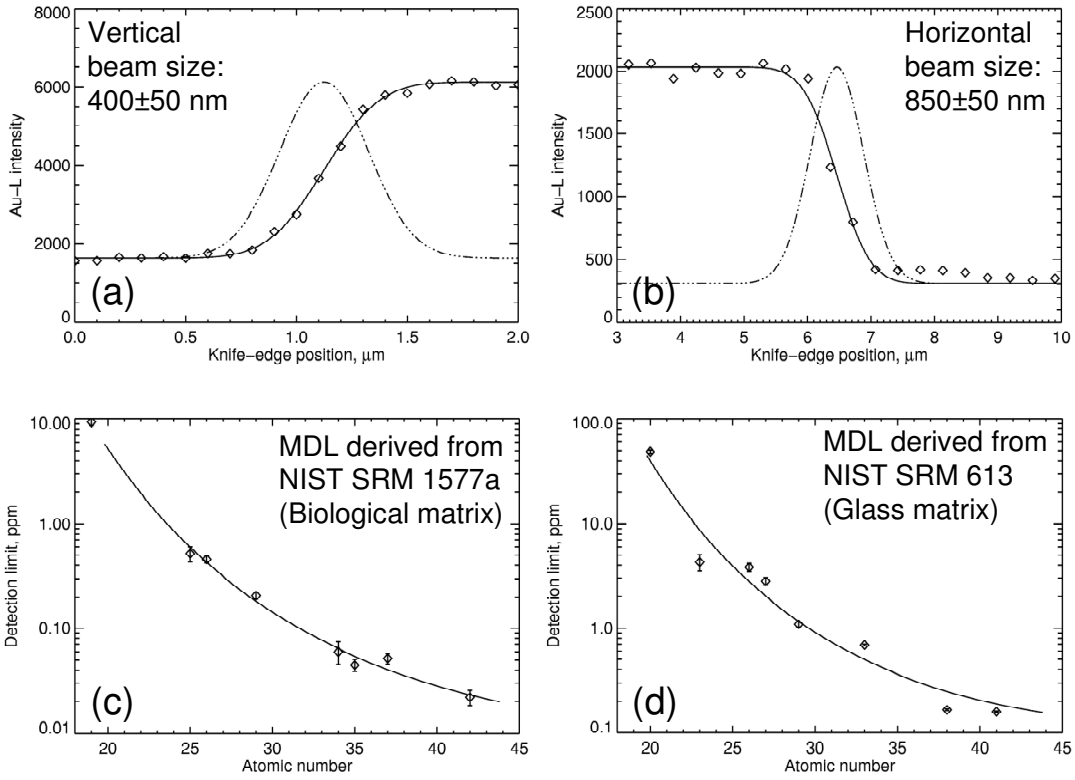

Fig. 2. Analytical characteristics achievable with SU-8 CRL lenses at ID18F: (a) vertical and (b) horizontal beam size; relative minimum detection limits for transition elements present in (c) a carbon-based and (d) a silica-based matrix.

3. Milestone 2. 2D/3D elemental analysis and scanning μ-XRD of diamond inclusions from Juina (Mato Grosso, Brazil) and from Koffiefontein (South-Africa) diamonds at the ID18F beam line.

3.1 Juina diamonds

The most unexpected finding in the deep mantle diamonds sofar was the detection of several syngenetic carbonate inclusions from Juina. The existence syngenetic carbonates was unexpected and is demonstrated in Fig. 3. Moreover, these represent the secondmost frequent inclusion-type found in this suite of ultradeep diamonds. Carbonates were detected in six diamonds (No. RS-05, 30, 35, 59, 63, 68), and in three diamonds (No. RS-35, 59, 68) we found several individual carbonate crystals. The identified carbonates typically have a white colour and are mostly very small, less than 20 μm in diameter. The largest crystal found was about 50 μm.

In Fig. 3, the shape, orientation and crystallinity of a two syngenetic inclusions found in one of the Juina diamonds are shown. We could show through a combination of confocal μ-XRF+μ-XRD (see Fig. 3C) and confocal Raman microscopy that inclusion A contains calcite while inclusion B contains walstromite-structured $CaSiO_3$. Pure Ca-silicate inclusions indicate a lower mantle origin of the diamond. Both inclusions show an identical shape and orientation which is diagnostic for their syngenetic origin. Around some of the crystals, a dark halo, rich in rare-earth elements (REE) was observed.

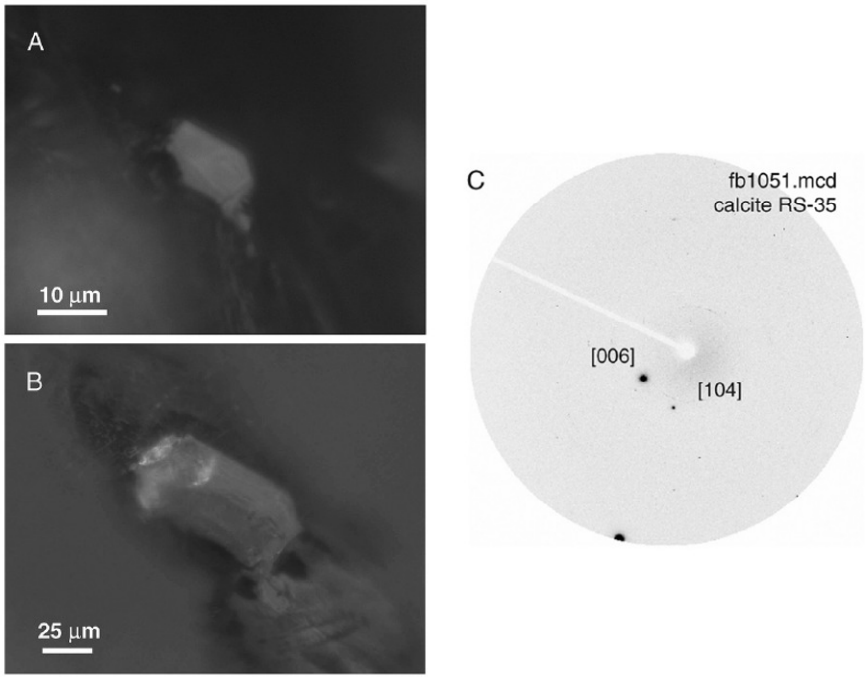

Fig. 3 (A) Syngenetic calcite inclusion, (B) syngenetic walstromite structured $CaSiO_3$ inclusions in a Juina diamond, (C) XRD image corresponding to A.

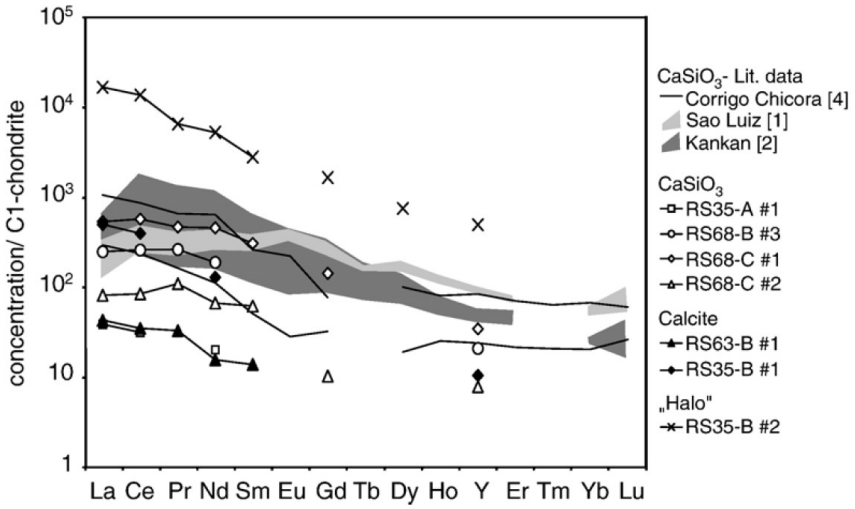

Fig. 4. REE patterns of four walstromite-structured $CaSiO_3$ (open symbols), two calcite (filled symbols) inclusions and a "halo" (crosses) surrounding a calcite inclusion. Published REE patterns of lower mantle $CaSiO_3$-inclusions are also shown.

X-ray diffraction mapping of individual inclusions demonstrates that all carbonates are single crystals (Fig. 3C) which excludes a pseudomorphic replacement of former syngenetic inclusions by late stage epigenetic carbonates. All late stage carbonates so far identified in diamonds from other locations are typically polycrystalline aggregates with sub-micron grain size and found in surface fractures.

The quantitative evaluation of the measured 3D-XRF data-set was performed in two steps. A K-means clustering algorithm was applied first in order to mathematically separate the major phases and calculate their corresponding (average) XRF spectra. This procedure was followed by a fundamental parameter scheme to convert the spectral line intensities into elemental concentrations.

In Fig. 4 the REE-patterns of some of the Ca-rich inclusions are shown in comparison to published REE-patterns of lower mantle $CaSiO_3$-inclusions. All measured phases display similar types of REE patterns. The obtained patterns show strong enrichment of LREE decreasing gradually towards heavier REE, which is similar to published REE contents of lower mantle $CaSiO_3$ phases found worldwide (Sao Luiz, Kankan, Corrigo Chicora). The mean enrichment is around 100 times C1 chondrite. The halo yields the highest REE content, of up to 10,000 times chondritic followed by walstromite-structured $CaSiO_3$ inclusions and the carbonates. Calcite and walstromite-structured $CaSiO_3$ phases coexisting within the same diamond yield nearly identical REE-pattern, with calcite showing higher values. Absorption of the diamond host prevents the in situ detection of REE at lower concentration levels.

The observed imposition of the dominant crystallographic faces of the diamond on the inclusions strongly supports a syngenetic or protogenetic origin. The occurrence of carbonates as single crystals negates the possibility of the calcite being a secondary, epigenetic alteration product or crystallized from a trapped carbonatitic melt.

A paper describing how these and related findings can be interpreted as pointing to the presence of a substantial carbonate reservoir at great depth, was recently published in ESPL, the leading journal for this type of investigations.

In summary, our finding demonstrates the extension of the CO_2 cycle to great depths which has consequences on the storage capicity of this important greenhouse gas over time.

F.E. Brenker, C. Vollmer, L. Vincze, B. Vekemans, A. Szymanski, K. Janssens, I. Szaloki, L. Nasdala, W. Joswig, F. Kaminsky, "Carbonates from the lower part of transition zone or even the lower mantle", Earth and Planetary Science Letters, 260 (2007) 1-9

3.2 **Milestone 3** *Koffiefontein diamonds (A reference frame for "normal" shallow mantle fluids)*

In the figures below, some typical results of the ID18F measurement sessions on *Koffiefontein* (South Africa) diamonds, which involve the explorative scanning of single inclusions or clouds of inclusions by means of confocal μ-XRF, are shown. From the elemental maps that are collected, it seems that within such a cloud, a wide variety of inclusion compositions is present.

Next to regions rich in Fe and Ni, another type of inclusion exists that is rich in Ca, Mn, Fe, Cu, Sr, Zr, Nb; high fluorescent intensities of these elements can be observed. In a third type of inclusion, the element K is more abundantly present than Ca, next to Fe, Cu, Pb and Sr. The fact that there are three (or more) types of inclusions that seem to occur simultaneously in the same diamond, in close proximity to one another, contradicts current models of fluid miscibility at the depth of formation of these diamonds. Fluids of very different composition should not co-exist in close proximity. In order to prove without any doubt and document better the co-existence of the different types of fluids in Finsch and Koffiefontein diamonds, an investigation by the means of high resolution techniques at ID22NI was performed (see Milestone 4). These data are important and exciting in their own right but the study of lithospheric cloudy diamonds from Finsch and Koffiefontein is also a reference frame for follow-up studies on fluid inclusions in deep diamonds from Juina and Kankan that were just recently detected by our group; these diamonds sample the Earth down to the lower mantle.

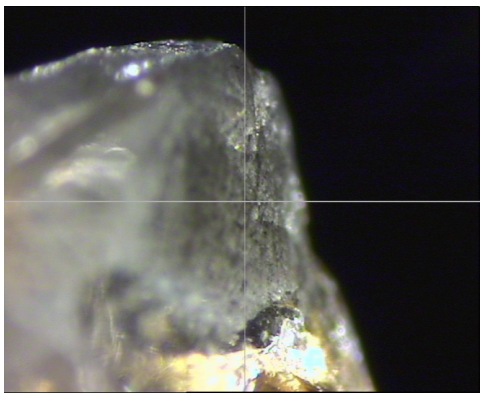

Fig. 5. Optical micrograph of raw diamond (Kf 07-4, from *Koffiefontein*, South Africa) showing a cloud of small inclusions close to the surface.

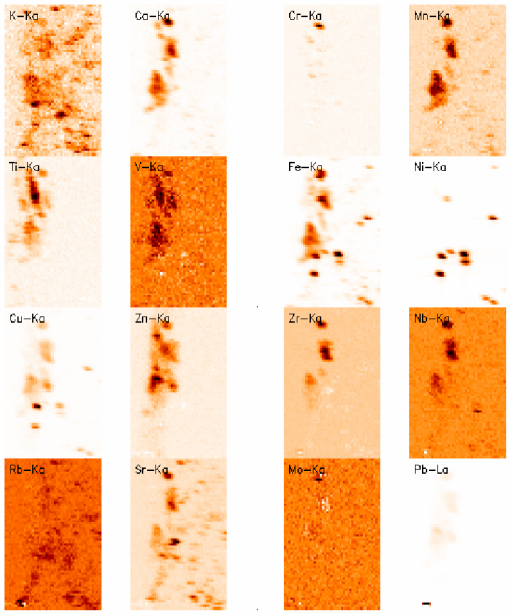

Fig. 6. Elemental maps in a virtual plane inside the diamond of Fig. 5 showing different elemental compositions in different inclusions.
Image size: 46x66 μm^2. Pixel size is 1x1 μm^2.

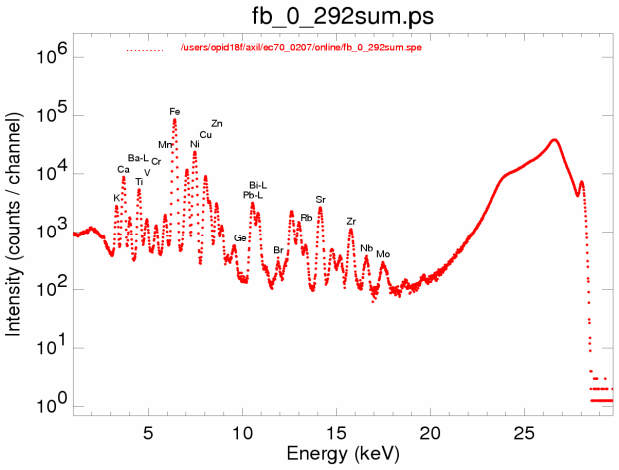

Fig. 7. Sum XRF spectrum corresponding to the elemental maps shown in Fig. 4.

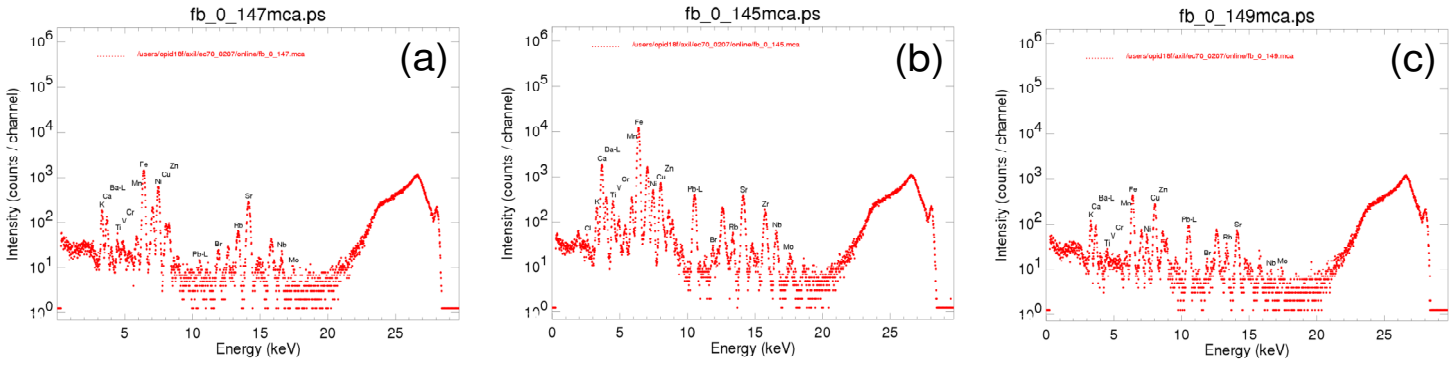

Fig. 8. Confocal-XRF spectra of (a) Fe, Ni-rich inclusions, (b) Ca, Mn, Fe-rich inclusions, (c) K, Fe, Cu, Pb-rich inclusions.

Table 1. Calculated elemental concentrations corresponding to the XRF-spectra shown in Fig. 8. The estimated uncertainty of the indicated concentration values varies between 20-30 %, mostly originating from the uncertainties associated with the estimation of the irradiated inclusion volumes.

Element	Fb_0_147.mca Inclusion type (a)	Fb_0_145.mca Inclusion type (b)	Fb_0_149.mca Inclusion type (c)
K (%)	1.1	1.3	0.60
Ca (%)	0.8	**14.5**	0.55
Ti (%)	0.006	0.4	0.013
V (ppm)	50	500	30
Cr (ppm)	70	300	60
Mn (%)	0.01	**0.1**	0.005
Fe (%)	0.3	**2.5**	0.10
Ni (ppm)	**550**	**400**	50
Cu (ppm)	60	520	210
Zn (ppm)	19	110	50
Rb (ppm)	40	25	15
Sr (ppm)	170	240	40
Zr (ppm)	< DL	80	< DL
Nb (ppm)	15	40	5
Mo (ppm)	15	15	20
Pb (ppm)	10	640	150

4. Milestone 4. 2D/3D elemental analysis of very small fluid inclusions in shallow mantle diamonds at the ID22NI beam line.

In Fig. 9 and 10, a summary of the results of performing a confocal μ-XRF experiment at the ID22NI beamline of ESRF is presented. The nanobeam, produced by means of KB-optics, of dimensions 125x165 nm^2, induced X-ray fluorescence in a narrow tunnel of matter; of this tunnel, a length of 16 μm long was visible to the EDXRF detector via the use of a polycapillary lens in between sample and detector. In Fig. 9 the absolute and relative detection limits obtained by measuring the standard reference materials NIST SRM 613, 1833 (Trace Elements in Glass) and 1577a (Bovine Liver) are shown. Relative and absolute detection limits of resp. 0.1 ppm and 0.1 fg were reacheable.

This setup was employed to record the submicroscopic distribution of trace elements in/near a series of very small fluid inclusions in *Koffiefontein* diamonds in a number of areas of 10x10 μm^2 wide. The fact that a nanometric X-ray beam is available at ID22NI allow to record detailed maps of the distribution of key elements, such as K, Ca and Ni, corresponding to the three categories of "inclusions" previously established at a coarser resolution level (ID18F – see Milestone 3). Some of the results obtained are shown in Fig. 10.

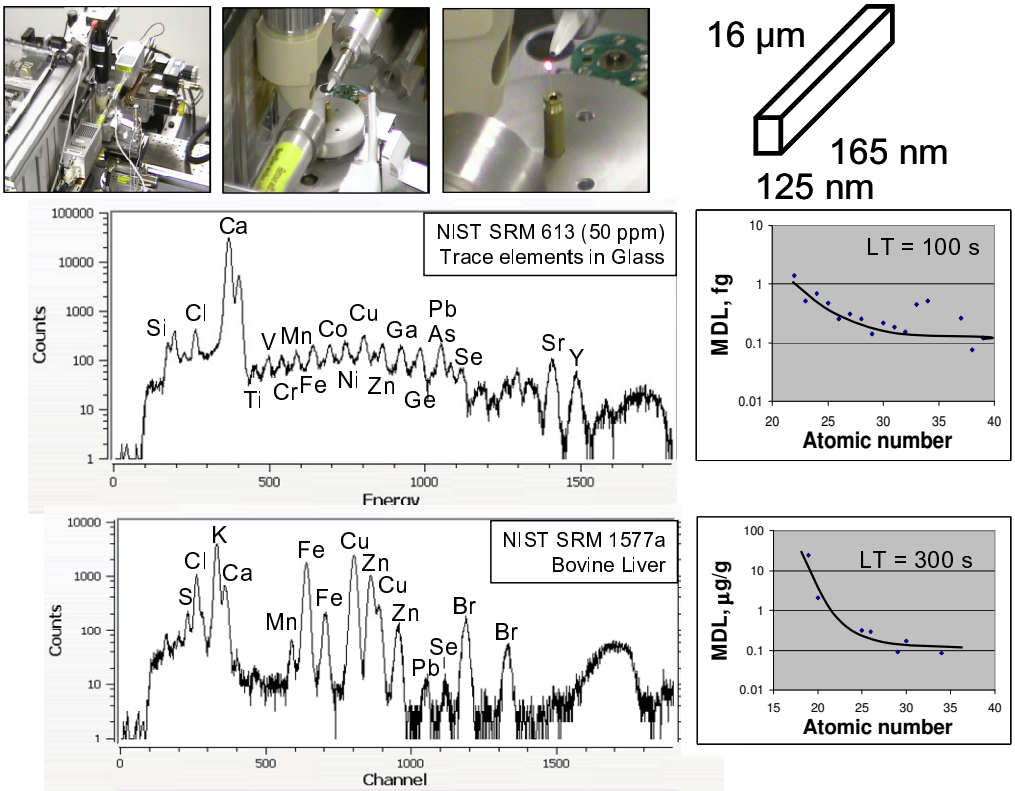

Fig. 9. Confocal XRF spectra of calibration standards and detection limit values derived from these obtained at ID22NI.

Similarly as in the maps of Fig. 5, next to the inclusions *per se,* also broader streaks of specific elements are visible. A possible interpretation of these structures is that they are the result of the precipitation of salts from fluids that have filled cracks in the diamond. What is also striking is that the small regions of one type (e.g., the K-rich type), frequently appear to be very close to regions of another type or that both regions are in fact parts of a single inclusion. Possibly this is caused by the crystallisation of different phases (with different compositions) in various sub-volumes of the same inclusion. This appears to be most frequently the case for the K and Ca-rich inclusions. Thus, the most likely interpretation is that the fluid composition in the abovementioned region of diamonds start with a single Ca- and K-composition. After the fluid is trapped during growth of the diamond, Ca-rich phases starts crystallize first (as predicted from model calculations). The crystallisation of Ca-rich phases causes the Ca-content of the remaining fluid to decrease. Under certain circumstances Ti and/or Cr-rich mineral phases crystallizes as well. The remaining fluid composition becomes richer in K and other incompatible elements.

It can be concluded that the nanoscopic view we gained during the 2007/I experiment certainly has shed a completely different light on the “fluid”-inclusions study. Now the reference frame is set and unique deeper mantle fluids can be studied.

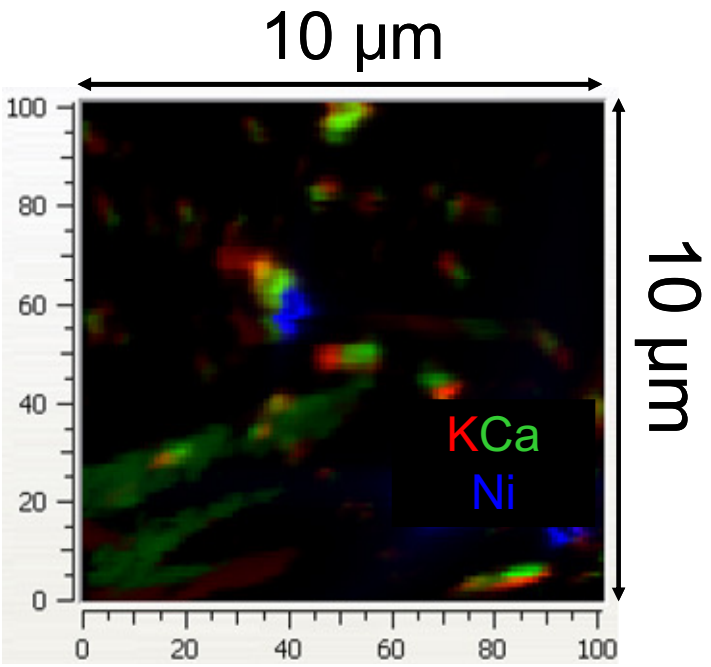

Fig. 10. High resolution RGB-map of the K, Ca and Ni intensity of a series of micrometer-sized inclusions immediately below the surface of a *Koffiefontein* diamond.

In the second half of the LT proposal period, we plan to continue with this type of measurements, in order to intercompare the inclusions diamonds from shallow sources (Finsch, Koffiefontein) with diamonds from the deep asthenospheric mantle down to the transition zone (410-670km) and lower mantle (>670km depth) (Juina, Kankan). This will be the first time that captured fluids from such depths can be studied directly and will provide important insights into the global fluid transport and budget, as well as on the nature of deep mantle fluids.

5. Conference presentations

K. Janssens, "Confocal μ-XRF and absorption/diffraction-tomography: three-dimensional methods suitable for non-destructive analysis of heterogeneous multiphase materials", (invited lecture), EMRS Spring 2007 meeting, 28 May-1 June 2007, Strasbourg, France.

F.E. Brenker, Vincze, L., Vekemans, B., Janssens, K. & Harris, J. "The relationship between inclusions and diamond host", (invited lecture). - De Beers diamond conference, Cambridge, 2006.

F.E. Brenker, Vollmer, C., Vincze, L., Vekemans, B., Szymanski, A., Janssens, K., Szaloki, I., Nasdala, L., Joswig, W. & Kaminsky, F. "CO_2-recycling to the deep convecting mantle." - Goldschmidt Conference, Melbourne, 2006.

K. Janssens, "Combined use of conventional and confocal μ-XRF and μ-XANES, μ-XRD, X-ray absorption tomography and Raman spectrometry for speciation analysis in two and three dimensions", (invited lecture), Denver X-ray Conference, Colorado Springs, CO, US, 30 July-3 August 2007.

K. Janssens, "Three-dimensional elemental and phase analysis", (invited lecture), International Congress on X-ray Optics and Microanalysis, Kyoto, Japan, 17- 20 September 2007.

K. Janssens, "Non-destructive analysis and speciation of heavy metals in environmental and biological materials by means of a combination of hard X-ray microprobe techniques" (plenary lecture) 4th APICPAC (Asia-Pacific Symposium on Pollutants' Analysis and Control), Beijing, P.R. China, 10-15 October 2007.

K. Janssens, "Analysis of materials at different length-scales" (plenary lecture), HASYLAB User's meeting, Hamburg, Germany, 25 January 2008.

K. Janssens, "Analysis of materials at different length-scales" (plenary lecture) AXAA2008 (Australian X-ray Analysis Association meeting), Melbourne, Australia, 2-5 February 2008.

F.E. Brenker, Vincze, L., Vekemans, B., Szymanski, A., De Nolf, W., Janssens, K., Stachel, T. & Harris, J. "Detection of a REE-rich, F- and P-bearing fluid component in superdeep diamonds from Kankan (Guinea)" – 9IKC, Frankfurt, 2008.

T. Pisternick, Silversmit, G., Schoonjans, T., Brenker, F.E., Vincze, L., Vekemans, B., De Nolf, W., Janssens, K. & Harris, J. "S-XRF and XANES Analysis of Fluid-Inclusions in Cloudy Diamonds from Koffiefountein and Finsch" – 9IKC, Frankfurt, 2008.

F.E. Brenker, Vincze, L., Vekemans, B., Szymanski, A., Janssens, K. & Kaminsky, F. (2008) Detection of a new REE-rich, F- and P-bearing deep mantle fluid. - Earth and Planetary Science Letters (in Preparation).